Computers & Geosciences 102 (2017) 109–115

Contents lists available at ScienceDirect

Computers & Geosciences

journal homepage: www.elsevier.com/locate/cageo

Case study

Effects of acid dissolution capacity on the propagation of an acid-dissolution front in carbonate rocks

Chongbin Zhao[a,*], B.E. Hobbs[b], A. Ord[b]

[a] Central South University, Computational Geosciences Research Centre, Changsha 410083, China
[b] The University of Western Australia, School of Earth and Environment, Perth, WA 6009, Australia

ARTICLE INFO

Keywords:
Acidization
Front propagation
Carbonate rocks
Numerical solutions
Acid dissolution capacity

ABSTRACT

Acid dissolution capability plays a considerable role in controlling the propagation of an acid-dissolution front in the carbonate rocks that are saturated by pore fluids. This capability can be represented by a dimensionless number, known as the acid dissolution capability number, by which we mean the quotient of the volume of an acid-dissolved carbonate rock divided by that of the acid itself. This paper aims primarily to investigate why and how the acid dissolution capacity can affect the behaviors of the acid-dissolution front propagation in the carbonate rocks that are saturated by pore fluids. If the acid dissolution capacity number is a nonzero finite number, as in a general case, then the computational simulation method needs to be employed to get numerical solutions for the acid-dissolution system. The relevant computational simulation results have demonstrated that: (1) with an increase in the value of the Zhao number (namely another dimensionless number), which is used to denote the dynamic characteristics of an acid-dissolution system, the acid-dissolution front becomes more unstable in the corresponding supercritical acid-dissolution system. (2) When the acid dissolution capacity number is small enough, the propagating speed of a planar acid-dissolution front in the corresponding subcritical acid-dissolution system is linearly dependent on the acid dissolution capacity number, indicating that the smaller the acid dissolution capacity, the slower the propagating speed of a planar acid-dissolution front in the corresponding subcritical acid-dissolution system. (3) With a decrease in the acid dissolution capacity number, the acid-dissolution front can exhibit more unstable behavior in the corresponding supercritical acid-dissolution system.

1. Introduction

Acid dissolution capability plays a considerable role in controlling the propagation of an acid-dissolution front in the carbonate rocks that are saturated by pore fluids. This phenomenon is closely associated not only with developing innovative techniques for efficiently extracting oil/gas resources in carbonate rocks within the deep Earth (Sherwood, 1987; Hinch and Bhatt, 1990; Fredd and Fogler, 1998; Golfier et al., 2002; Panga et al., 2005; Kalia and Balakotaiah, 2007, 2009; Cohen et al., 2008), but also with understanding the dominating dynamic mechanisms for controlling the formation of large ore deposits within the Earth's upper crust (Chadam et al., 1986, 1988; Ormond and Ortoleva, 2000; Ortoleva et al., 1987; Chen and Liu, 2002, 2004; Zhao et al., 2008; Chen et al., 2009). Since acid dissolution can create the porosity of a carbonate rock, it may lead to a significant variation in the channels of the carbonate rock. As a result, the flow patterns of pore fluids in the carbonate rock can change dramatically. This means that the propagation of an acid-dissolution front depends on both the chemical dissolution reaction process and the physical processes associated with the flow of pore fluids. Generally, the evolution of an acid-dissolution front is controlled by a dynamic interaction among the following three processes, namely mass diffusion, advection (caused by the flow of pore fluids) and acid dissolution reaction processes, which take place simultaneously in the carbonate rocks that are saturated by pore fluids. This dynamic interaction can be reflected by the Zhao number (i.e. a dimensionless number), which is used to denote the dynamic characteristics of an acid-dissolution system (Lai et al., 2016; Zhao et al., 2009). Because the studies of acid-dissolution front propagation problems have considerable scientific significance and potential application background, extensive research has been conducted in this particular field (Sherwood, 1987; Hinch and Bhatt, 1990; Fredd and Fogler, 1998; Golfier et al., 2002; Panga et al., 2005; Kalia and Balakotaiah, 2007, 2009; Cohen et al., 2008; Lai et al., 2016; Zhao et al., 2009, 2013a, 2013b).

The existing research outcomes on the propagation of an acid-dissolution front in the carbonate rocks (that are saturated by pore

* Corresponding author.
E-mail address: Chongbin.zhao@iinet.net.au (C. Zhao).

http://dx.doi.org/10.1016/j.cageo.2017.02.013
Received 5 April 2016; Received in revised form 20 October 2016; Accepted 16 February 2017
Available online 20 February 2017
0098-3004/

fluids) have demonstrated that: (1) the acid-dissolution front can have one of the following three states: stable, critical and unstable, which are in correspondence to subcritical, critical and supercritical acid-dissolution systems respectively; (2) only in a subcritical (or even critical) acid-dissolution system, the (planar) acid-dissolution front does not change its shape during propagation, so that a moving coordinate system, in which the subcritical acid-dissolution system can be viewed as being in a steady-state, is usable in the related theoretical analysis; (3) when an acid-dissolution system is in a supercritical state, it is currently impossible to describe the shape evolution of an acid-dissolution front with time in a purely mathematical manner, so that computational simulation methods should be employed for simulating the shape evolution of an acid-dissolution front with time. This means that in order to consider more general cases of an acid-dissolution front propagating problem, the mixed approach consisting of both the finite difference and finite element methods needs to be used as a research tool in this study (Lai et al., 2016; Zhao et al., 2009, 2013a, 2013b).

In order to effectively and efficiently solve acid-dissolution front propagating problems in the carbonate rocks that are saturated by pore fluids, it is necessary to transform the related mathematical governing equations from a dimensional form into a dimensionless one. In the process of conducting this mathematical transformation, the scaling parameters should be carefully chosen to avoid any mathematical indefinite problem of zero-over-zero type. Consequently, different values (including zero) of the acid dissolution capacity number can be considered for investigating the effects of acid dissolution capacity on the propagation of an acid-dissolution front in the carbonate rocks, which are saturated by pore fluids. Since this issue has not been addressed up to date, it becomes the main purpose of carrying out this study. The outcome of this study will answer the following realistic question: why and how can acid dissolution capacity affect the propagation of an acid-dissolution front in the carbonate rocks (that are saturated by pore fluids) in the case of the acid-dissolution system under consideration is in a supercritical state?

2. Mathematical governing equations and related analysis

From the previous studies (Zhao et al., 2013a, 2013b), the mathematical governing equations for describing the propagation problem of an acid-dissolution front in carbonate rocks, which are saturated by pore fluids, can be written as follows:

$$\vec{u} = -\frac{K(\phi)}{\mu}\nabla p \tag{1}$$

$$\frac{\partial \phi}{\partial t} + \nabla\bullet\vec{u} = 0 \tag{2}$$

$$\frac{\partial}{\partial t}(\phi C) + \nabla\bullet(C\vec{u}) = \nabla\bullet(\phi D\nabla C) - sk\ C \tag{3}$$

$$\frac{\partial \phi}{\partial t} = \frac{\chi}{\rho_s} sk\ C \tag{4}$$

$$\gamma_a = \frac{C_{in}\chi}{\rho_s(\phi_f - \phi_0)} \tag{5}$$

where p is used to denote the pore-fluid pressure; $\vec{u}$ is used to denote the Darcy velocity vector associated with the acid-dissolution system; C is used to denote the acid concentration (that has a unit of moles per pore-fluid volume); ϕ is used to denote the carbonate rock porosity; μ is used to denote the pore-fluid dynamic viscosity; $K(\phi)$ is used to denote the carbonate rock permeability; D is used to denote the acid diffusivity/dispersivity; χ is used to denote the carbonate rock stoichiometric coefficient; k is used to denote the rate constant with a unit of m/s; s is used to denote the reactive surface area per unit volume of the dissolvable mineral; C_{in} is used to denote the injected acid concentration (i.e. moles per pore-fluid volume) at the entrance of the acid-dissolution system; ρ_s is used to denote the carbonate rock molar density (with a unit of moles per volume); γ_a is used to denote the acid dissolution capacity number, which is defined as the ratio of the volume of an acid-dissolved carbonate rock to that of the acid itself.

For the purpose of considering the carbonate rock permeability change resulted from a variation in the corresponding carbonate rock porosity, it is very common to employ the Carman-Kozeny law (Scheidegger, 1974; Nield and Bejan, 1992) for calculating the carbonate rock permeability, K, for a given carbonate rock porosity, ϕ.

$$K(\phi) = \frac{K_0(1-\phi_0)^2\phi^3}{\phi_0^3(1-\phi)^2} \tag{6}$$

where ϕ_0 is used to denote the initial reference porosity of the carbonate rock; K_0 is used to denote the corresponding initial reference permeability of the carbonate rock.

To identify the leading terms in the above-mentioned mathematical governing equations, it is necessary to transform Eqs. (1)–(4) from a dimensional form into a dimensionless one. This requires the use of both the time scale and the length scale, which should reflect or represent the primary dimensions of the physical problem under consideration. However, since real acid-dissolution systems are typically unbounded, this means that the geometrical length (i.e. the geometrical dimension) of them is infinite, which is certainly unsuitable to be used as the length scale. In this situation, it is necessary to examine the definition of the Peclet number, which is used to express the relative dominating process between the mass advection and diffusion processes, and the definition of the Damkuhler number, which is used to express the relative dominating process between the mass advection and chemical reaction processes.

$$Pe = \frac{v_{fluid}L_c}{D_0}, \quad Da = \frac{ks_0L_c}{v_{fluid}} \tag{7}$$

where Pe is the Peclet number of the acid-dissolution system; Da is the Damkuhler number of the acid-dissolution system; s_0 is used to denote the reference reactive surface area per unit volume of dissolvable minerals; v_{fluid} is used to denote the injected pore-fluid velocity at the entrance of the acid-dissolution system; D_0 is used to denote the acid effective diffusivity/dispersivity; L_c is used to denote the characteristic length of the acid-dissolution system. Note that L_c is usually chosen as the pore size for pore scale models (Golfier et al., 2002), and as the sample size for the Darcy scale models (Kalia and Balakotaiah, 2007, 2009).

Eq. (7) clearly indicates that since either the Peclet number or the Damkuhler number cannot represent three main processes (i.e. the mass advection, diffusion and chemical reaction processes), which take place simultaneously in an acid-dissolution system, it is desirable to define a new dimensionless parameter as follows:

$$H = \frac{Da}{Pe} = \frac{ks_0D_0}{(v_{fluid})^2} \tag{8}$$

Eq. (8) indicates that the use of this new dimensionless number has the following two main advantages: (1) it is independent of the characteristic length of an acid-dissolution system, so that any finite numbers except zero can be used as the length scale, from the mathematical point of view; and (2) it can be used to represent the dynamic interaction among the mass advection, diffusion and chemical reaction processes, which take place simultaneously in an acid-dissolution system, so that it represents the characteristics of an acid-dissolution system in a much better way than either the Peclet number or the Damkuhler number does. Therefore, instead of either the Peclet number or the Damkuhler number, the new dimensionless parameter, H, which is equivalent to the Zhao number (as demonstrated later), is used in this investigation. Based on the above-mentioned recognition, the specific time and length scales (that are used in this study) are as follows:

$$t^* = \frac{1}{\gamma_a^{ref} ks_0}, \quad L^* = \frac{v_{fluid}}{ks_0} \tag{9}$$

where t^* and L^* are used to denote the time and "length" scales respectively; γ_a^{ref} is used to denote the reference acid dissolution capability number, which can be defined as:

$$\gamma_a^{ref} = \frac{C_{ref}\chi}{\rho_s(\phi_f - \phi_0)} \tag{10}$$

where C_{ref} is used to denote the non-zero reference acid concentration.

It should be pointed out that since L^* is a "length" scale, rather than the characteristic length (i.e. L_c) of the acid-dissolution system, it cannot be used in the definition of both the Damkuhler number and the Peclet number of the acid-dissolution system. This means that in general cases, L^* is not equal to L_c. However, in a special case, where the Damkuhler number of the acid-dissolution system is equal to unity, then L^* is equal to L_c. Thus, the physical meaning of L^* can be explained as follows: if L^* is taken as the characteristic length (i.e. L_c) of an original acid-dissolution system (expressed in the original coordinate system), then the Damkuhler number of the transformed acid-dissolution system could be equal to unity in the transformed coordinate system.

Comparison of Eq. (5) with Eq. (10) leads to the following mathematical relationships:

$$\gamma_a = \alpha\gamma_a^{ref}, \quad \alpha = \frac{C_{in}}{C_{ref}} \tag{11}$$

By using the proposed time and "length" scales, the dimensionless governing equations for describing the acid dissolution problem in the carbonate rocks (that are saturated by pore fluids) can be derived and expressed as follows:

$$\gamma_a^{ref}\frac{\partial\phi}{\partial\bar{t}} + \bar{\nabla}\bullet\vec{\bar{u}} = 0 \tag{12}$$

$$\gamma_a^{ref}\frac{\partial}{\partial\bar{t}}(\phi\bar{C}) + \bar{\nabla}\bullet(\bar{C}\vec{\bar{u}}) = \frac{ks_0D_0}{(v_{fluid})^2}\bar{\nabla}\bullet(\frac{\phi}{\phi_f}\bar{\nabla}\bar{C}) - \bar{s}\,\bar{C} \tag{13}$$

$$\frac{\partial\phi}{\partial\bar{t}} = (\phi_f - \phi_0)\bar{s}\bar{C} \tag{14}$$

The related dimensionless quantities in these equations are defined below:

$$\bar{t} = \frac{t}{t^*}, \quad \vec{\bar{u}} = \frac{\vec{u}}{v_{fluid}}, \quad D_0 = \phi_f D \tag{15}$$

$$\bar{C} = \frac{C}{C_{ref}}, \quad \bar{x} = \frac{x}{L^*}, \quad \bar{y} = \frac{y}{L^*} \tag{16}$$

$$\bar{s} = \frac{s}{s_0} = \frac{\phi_f - \phi}{\phi_f - \phi_0} \tag{17}$$

$$\vec{\bar{u}} = -\frac{K(\phi)}{K(\phi_f)}\bar{\nabla}\bar{p}, \quad \bar{\nabla}\bar{p} = \frac{\nabla p}{(\nabla p)^*},$$
$$(\nabla p)^* = -\frac{\partial p}{\partial x} = \frac{v_{fluid}\,\mu}{K(\phi_f)} \tag{18}$$

Note that the main advantage of using the unchanged time and length scales in this study is that the mathematical indefinite problem of zero-over-zero type can be avoided when the real acid dissolution capacity number approaches zero in an acid-dissolution system.

If the propagation problem of the acid-dissolution front under consideration has a rectangular computational domain, as shown in Fig. 1, then we can have the following corresponding boundary conditions:

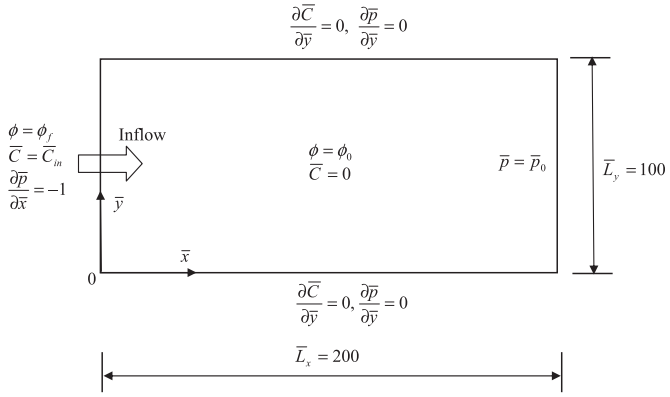

Fig. 1. Geometry and boundary conditions of the acid-dissolution front propagation problem in a fluid-saturated carbonate rock.

$$\bar{C}(\bar{x},\bar{y},\bar{t}) = \bar{C}_{in}, \quad \phi(\bar{x},\bar{y},\bar{t}) = \phi_f,$$
$$\frac{\partial\bar{p}(\bar{x},\bar{y},\bar{t})}{\partial\bar{x}} = -1.0 \quad (\text{at } \bar{x} = 0) \tag{19}$$

$$\frac{\partial\bar{C}(\bar{x},\bar{y},\bar{t})}{\partial\bar{x}} = 0, \quad \bar{p}(\bar{x},\bar{y},\bar{t}) = \bar{p}_0 \quad (\text{at } \bar{x} = \bar{L}_x), \tag{20}$$

$$\frac{\partial\bar{C}(\bar{x},\bar{y},\bar{t})}{\partial\bar{y}} = 0, \quad \frac{\partial\bar{p}(\bar{x},\bar{y},\bar{t})}{\partial\bar{x}} = 0,$$
$$(\text{at } \bar{y} = 0 \text{ and } \bar{y} = \bar{L}_y) \tag{21}$$

where $\bar{p}_0$ is used to denote the dimensionless pore-fluid pressure, which may be assigned at the exit of the acid-dissolution system.

The initial conditions for the propagation problem of the acid-dissolution front under consideration are: $\phi(\bar{x},\bar{y},0) = \phi_0$ expect at $\bar{x} = 0$, where $\phi(0,\bar{y},\bar{t}) = \phi_f$; and $\bar{C}(\bar{x},\bar{y},0) = 0$ expect at $\bar{x} = 0$, where $\bar{C}(0,\bar{y},\bar{t}) = 1$.

When the acid-dissolution system is stable (or even neutral), a planar acid-dissolution front in the acid-dissolution system under consideration can propagate in an infinite domain without changing its shape (Zhao et al., 2013a, 2013b). In this case, the propagating speed of the planar acid-dissolution front can be determined by considering the mass balance of the injected acid within the acid-dissolution system.

$$\chi(v_{fluid}C_{in} - v_{front}\phi_f C_{in}) = v_{front}(\phi_f - \phi_0)\rho_s \tag{22}$$

where v_{front} is used to denote the propagating speed of the planar acid-dissolution front; other quantities have the same meanings as those mentioned previously.

It should be pointed out that when a planar acid-dissolution front propagates forwardly, it must consume some acid to fill the final pore space (i.e. ϕ_f) of the carbonate rock. Thus, the acid consumed to dissolve the dissolvable mineral space (i.e. $\phi_f - \phi_0$) of the carbonate rock should be equal to the difference between the injected acid (i.e. $v_{fluid}C_{in}$) and the acid consumed to fill the final pore space of the carbonate rock (i.e. $v_{front}\phi_f C_{in}$).

According to Eq. (22), the propagating speed of a planar acid-dissolution front in the acid-dissolution system is expressed as follows:

$$v_{front} = \frac{v_{fluid}C_{in}}{\phi_f C_{in} + (\phi_f - \phi_0)\frac{\beta_s}{\chi}} = \frac{v_{fluid}}{\phi_f + \frac{1}{\gamma_a}} \tag{23}$$

Eq. (23) clearly indicates that when the acid dissolution capacity number is small enough, the propagating speed of a planar acid-dissolution front in the corresponding acid-dissolution system is approximately equal to the product of the acid dissolution capacity number and the injected pore-fluid velocity at the entrance of the corresponding acid-dissolution system. In this scenario, the propagating speed of a planar acid-dissolution front in the corresponding

subcritical acid-dissolution system is linearly dependent on the acid dissolution capacity number, indicating that the smaller the acid dissolution capacity, the slower the propagating speed of a planar acid-dissolution front in the corresponding subcritical acid-dissolution system.

3. Numerical simulation results

When the acid dissolution capability number is a nonzero finite number, Eqs. (12)–(14) are the dimensionless mathematical governing equations that need to be solved. Since it is very difficult, if not impossible to solve them in a pure mathematical manner, it is desirable to solve them numerically. For this purpose, a mixing approach consisting of the finite difference and finite element method is proposed in this paper, because it was used successfully in previous studies (Zhao et al., 2009, 2013b). In the proposed mixing approach, the finite element method can be chosen for discretizing the computational space, but the finite difference method can be chosen for discretizing the computational time.

For the propagation problem of an acid-dissolution front in the acid-dissolution system, as shown in Fig. 1, it is assumed that the corresponding computational domain has a dimensionless width of 100 (i.e. $\overline{L}_y = 100$) and a dimensionless length of 200 (i.e. $\overline{L}_x = 200$). We use the following parameters in the forthcoming computational simulation of this problem. The carbonate rock initial porosity (i.e. ϕ_0) before the acid is injected into the acid-dissolution system and the carbonate rock final porosity (i.e. ϕ_f) when the dissolvable minerals in the carbonate rock under consideration are completely dissolved are 0.1 and 0.2. If the ratio of $\frac{\chi}{\rho_s}$ is assumed to be 0.001 $m^3/Kmole$ and the reference acid concentration is equal to 0.1 $Kmole/m^3$, then the reference acid dissolution capacity number (i.e. γ_a^{ref}) can be determined (from Eq. (10)) as 0.001. Except for the left boundary of the considered acid-dissolution system, the carbonate rock initial porosity is equal to 0.1, whereas the initial dimensionless acid concentration is zero in the considered acid-dissolution system. The carbonate rock final porosity is applied on the left boundary of the acid-dissolution system, so that it can serve as a boundary condition for the considered acid-dissolution system. For the purpose of considering the effect of different acid dissolution capacity number on the numerical simulation results, the dimensionless acid concentration, which can be viewed as a variable, needs to be applied on the left boundary of the considered acid-dissolution system. When the two dimensionless acid concentrations (that are used in this study) are equal to 1.0 and 100 respectively, the corresponding acid dissolution capacity numbers are equal to 0.001 and 0.1, which can be determined from Eq. (11). Since the dimensionless horizontal velocity (i.e. $\bar{v}_{fluid}$) of the injected pore fluid on the left boundary of the considered acid-dissolution system is equal to unity, the corresponding dimensionless pressure gradient of the pore fluid along this direction should be equal to −1.0. To adequately simulate the propagation of an acid-dissolution front in the considered acid-dissolution system, it is simulated by 50000 four-node rectangular elements with 52026 nodal points in total. Furthermore, three different values of H (in Eqs. (8) and (13)), namely 0.2, 1.0 and 4.0, are used to consider the corresponding effects on the numerical simulation results.

Figs. 2 and 3 show the numerical simulation results for the propagation of an acid-dissolution front in the carbonate rock (that is

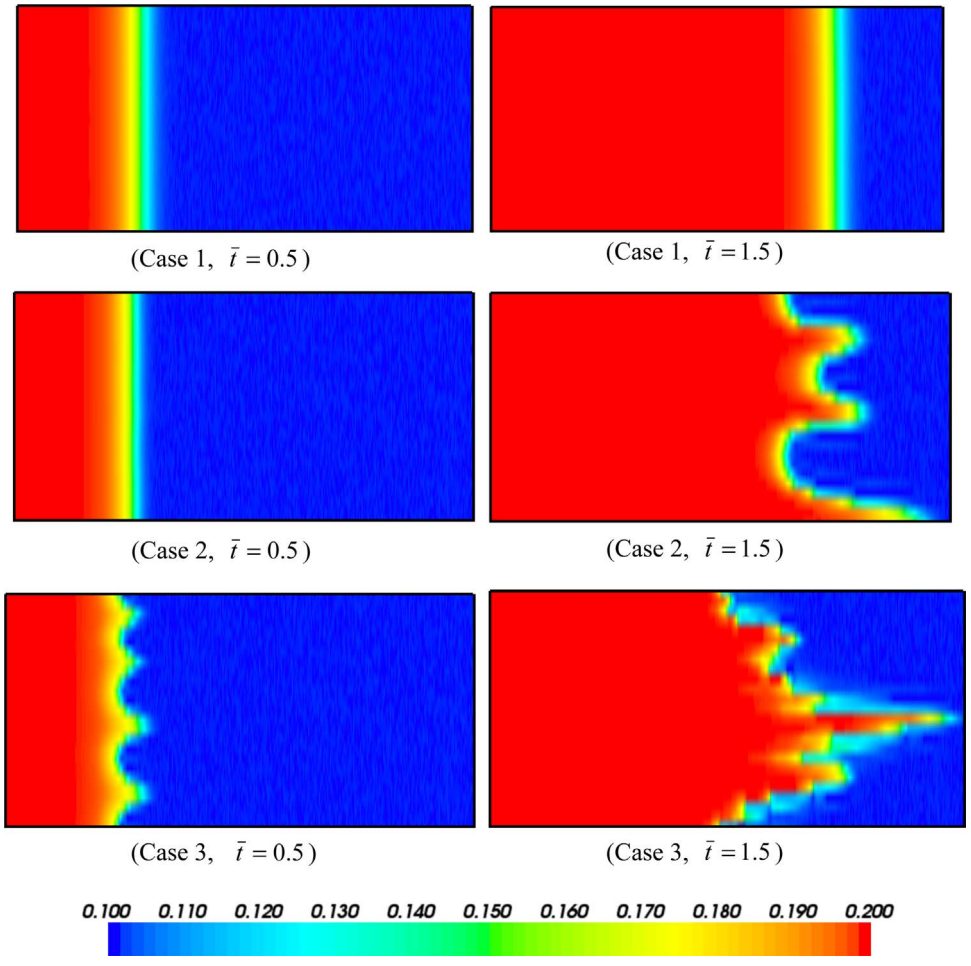

Fig. 2. Simulation results of the acid-dissolution front propagation problem in the fluid-saturated carbonate rock ($\gamma_a = 0.1$).

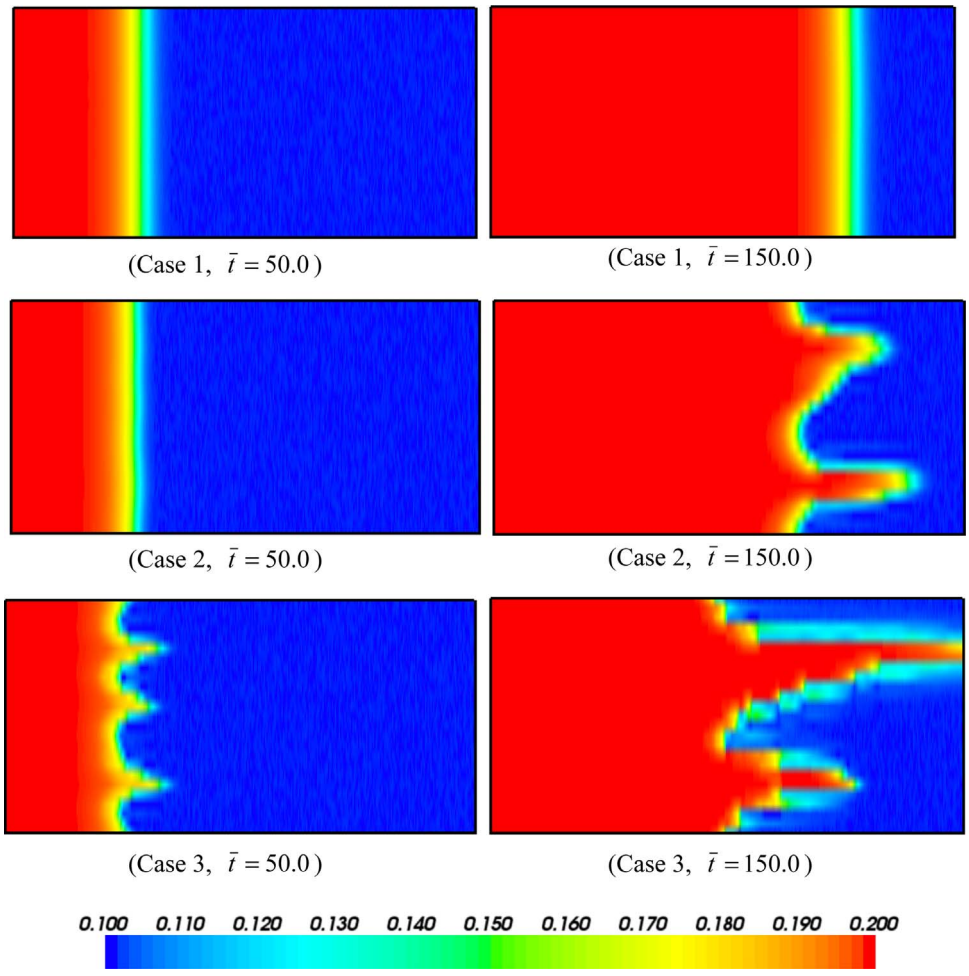

Fig. 3. Simulation results of the acid-dissolution front propagation problem in the fluid-saturated carbonate rock ($\gamma_a = 0.001$).

saturated by pore fluids) for $\gamma_a = 0.1$ and $\gamma_a = 0.001$ respectively. In these figures, cases 1, 2 and 3 are in correspondence to $H = 4.0$, $H = 1.0$ and $H = 0.2$. To simulate the acid-dissolution front appropriately, two different dimensionless time step-lengths, namely 0.1 and 10, are used in the case of $\gamma_a = 0.1$ and $\gamma_a = 0.001$ respectively. It can be seen that with a decrease in the value of H, the acid-dissolution front becomes more unstable, so that it evolves from a simple geometrical shape into a complicated geometrical one. With $\gamma_a = 0.1$ taken as an example, the acid-dissolution front has a planar shape when $H = 4.0$ at $\bar{t} = 1.5$, while it has a much more complicated shape when $H = 0.2$. Since H is a dimensionless comprehensive parameter (that is used for denoting the dynamic characteristics of an acid-dissolution system), it can be expressed by using the Zhao number (that is usually marked by Zh) of the same acid-dissolution system (Zhao et al., 2013a, 2013b). Through the comparison of their definitions, it can be found that $Zh = \frac{1}{\sqrt{H}}$. This indicates that with an increase in the value of the Zhao number, the considered acid-dissolution front becomes more unstable. Since this conclusion is consistent with the previous one, it can be concluded that the proposed mixing approach consisting of the finite difference and finite element method can produce useful numerical simulation results for dealing with the propagation problem of an acid-dissolution front in the carbonate rocks, which are saturated by pore fluids.

Note that with a decrease in the value of the acid dissolution capacity number, the propagation of an acid-dissolution front in the considered acid-dissolution system becomes much slower. For example, when the acid-dissolution front passes three quarters of the computational domain, the dimensionless time taken is equal to 1.5 when $\gamma_a = 0.1$, while the dimensionless time taken is equal to 150 when $\gamma_a = 0.001$. However, due to the specific velocity scale (i.e. Eq. (15)) used for this study, the simulated propagating speed of the acid-dissolution front in the computational model is much faster than the corresponding real propagating speed. This means that if two different velocity (speed) scales are used for the pore-fluid velocity and propagating speed of an acid-dissolution front, then caution should be taken in explaining the numerical simulation results. The velocity scale for injected pore-fluid flow in the considered acid-dissolution system is the pore-fluid velocity (i.e. v_{fluid}) at the entrance of the acid-dissolution system, while the velocity (speed) scale for the propagating speed of an acid-dissolution front in the considered acid dissolution system is $\gamma_a v_{fluid}$ during the process of deriving the dimensionless mathematical governing equations (that are expressed in Eqs. (12)–(14)) in this study. When the acid dissolution capacity number approaches zero, it is possible to find the relationship between the real and model dimensionless propagating speeds of an acid-dissolution front as follows:

$$\bar{v}^m_{front} = \frac{\gamma_a}{\gamma_a^{ref}}\bar{v}_{front} = \frac{\gamma_a}{\gamma_a^{ref}}\bar{v}_{fluid} = \frac{C_{in}}{C_{ref}}\bar{v}_{fluid} \tag{24}$$

where $\bar{v}^m_{front}$ is used to denote the model dimensionless propagating speed of an acid-dissolution front in the computational model; $\bar{v}_{front}$ is used to denote the real dimensionless propagating speed of the acid-dissolution front; $\bar{v}_{fluid}$ is used to denote the real dimensionless velocity of the injected pore-fluid flow in the acid-dissolution system. The same meanings have been used for other quantities, as mentioned previously.

Since the value of $\bar{v}_{fluid}$ is equal to unity, the theoretically predicted values for model dimensionless propagating speed of an acid-dissolution front within the computational model are equal to 100 and 1.0 in

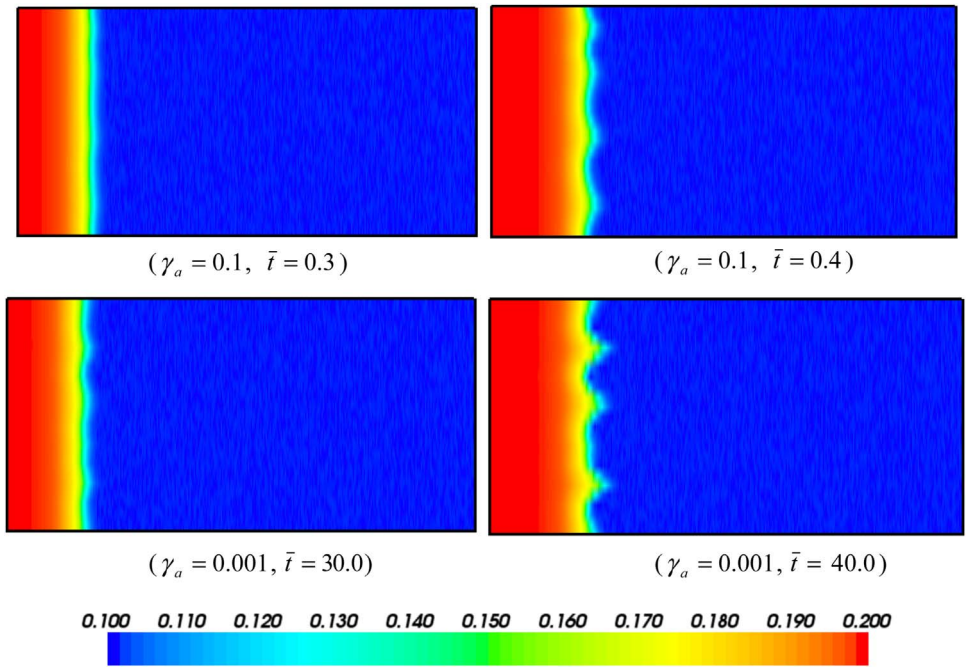

Fig. 4. Simulation results of the acid-dissolution front propagation problem in the fluid-saturated carbonate rock ($H = 0.2$).

the case of $\gamma_a = 0.1$ and $\gamma_a = 0.001$ respectively. These values can be directly obtained from Eq. (24). On the other hand, the numerically simulated values for model dimensionless propagating speed of the acid-dissolution front within the computational model are also about 100 and 1.0 in the case of $\gamma_a = 0.1$ and $\gamma_a = 0.001$ respectively. These values can be directly obtained from the computational simulation results (that are clearly displayed in Figs. 2 and 3). This further indicates that the suggested mixing approach consisting of the finite difference and finite element method can produce useful numerical simulation results for solving the propagation problem of an acid-dissolution front in the carbonate rocks, which are saturated by pore fluids.

As shown in Fig. 4, it can be also observed that when $H = 0.2$, the irregular shape of an acid-dissolution front grows slightly faster in the case of $\gamma_a = 0.001$ than it does in the case of $\gamma_a = 0.1$. This indicates that with a decrease in the acid dissolution capacity number, the acid-dissolution front can exhibit more unstable behavior in the corresponding supercritical acid-dissolution system.

4. Conclusions

In order to investigate why and how acid dissolution capability affect the propagation of an acid-dissolution front in the carbonate rocks (that are saturated by pore fluids), the related mathematical governing equations have been transformed from a dimensional form into a dimensionless form. In the process of carrying out this mathematical transformation, the corresponding scaling parameters are carefully chosen to avoid any mathematical indefinite of zero-over-zero type. This makes it possible to consider different values (including zero) of the acid dissolution capacity number in the related computational models, which can be safely employed for examining the effects of acid dissolution capacity on the propagation of an acid-dissolution front in the carbonate rocks, which are saturated by pore fluids.

The relevant computational simulation results have demonstrated the following: (1) with an increase in the value of the Zhao number, an acid-dissolution front can exhibit more unstable behavior in the corresponding supercritical acid-dissolution system. (2) When the acid dissolution capacity number is small enough, the propagating speed of a planar acid-dissolution front in a subcritical acid-dissolution system can be linearly dependent on the acid dissolution capacity number, indicating that the smaller the acid dissolution capacity, the slower the propagating speed of a planar acid-dissolution front in the corresponding subcritical acid-dissolution system. (3) With a decrease in the acid dissolution capacity number, the acid-dissolution front can also exhibit more unstable behavior in the corresponding supercritical acid-dissolution system.

Acknowledgements

This work is financially supported by the Natural Science Foundation of China (Grant No: 11272359). The authors express their thanks to the anonymous referees for their valuable comments, which led to a significant improvement over an early version of the paper.

References

Chadam, J., Hoff, D., Merino, E., Ortoleva, P., Sen, A., 1986. Reactive infiltration instabilities. IMA J. Appl. Math. 36, 207–221.
Chadam, J., Ortoleva, P., Sen, A., 1988. A weekly nonlinear stability analysis of the reactive infiltration interface. IMA J. Appl. Math. 48, 1362–1378.
Chen, J.S., Liu, C.W., 2002. Numerical simulation of the evolution of aquifer porosity and species concentrations during reactive transport. Comput. Geosci. 28, 485–499.
Chen, J.S., Liu, C.W., 2004. Interaction of reactive fronts during transport in a homogeneous porous medium with initial small non-uniformity. J. Contam. Hydrol. 72, 47–66.
Chen, J.S., Liu, C.W., Lai, G.X., Ni, C.F., 2009. Effects of mechanical dispersion on the morphological evolution of a chemical dissolution front in a fluid-saturated porous medium. J. Hydrol. 373, 96–102.
Cohen, C.E., Ding, D., Quintard, M., Bazin, B., 2008. From pore scale to wellbore scale: impact of geometry on wormhole growth in carbonate acidization. Chem. Eng. Sci. 63, 3088–3099.
Fredd, C.N., Fogler, H.S., 1998. Influence of transport and reaction on wormhole formation in porous media. AIChE J. 44, 1933–1949.
Golfier, F., Zarcone, C., Bazin, B., Lenormand, R., Lasseux, D., Quintard, M., 2002. On the ability of a Darcy-scale model to capture wormhole formation during the dissolution of a porous medium. J. Fluid Mech. 457, 213–254.
Hinch, E.J., Bhatt, B.S., 1990. Stability of an acid front moving through porous rock. J. Fluid Mech. 212, 279–288.
Kalia, N., Balakotaiah, V., 2007. Modeling and analysis of wormhole formation in reactive dissolution in carbonate rocks. Chem. Eng. Sci. 62, 919–928.
Kalia, N., Balakotaiah, V., 2009. Effect of medium heterogeneities on reactive dissolution of carbonates. Chem. Eng. Sci. 64, 376–390.
Lai, K.H., Chen, J.S., Liu, C.W., Yang, S.H., Steefel, C., 2016. Effect of medium permeability anisotropy on the morphological evolution of two non-uniformities in a geochemical system. Journal Hydrol. 533, 224–233.
Nield, D.A., Bejan, A., 1992. Convection in Porous Media. Springer-Verlag, New York.

Ormond, A., Ortoleva, P., 2000. Numerical modeling of reaction-induced cavities in a porous rock. J. Geophys. Res. 105, 16737–16747.
Ortoleva, P., Chadam, J., Merino, E., Sen, A., 1987. Geochemical self-organization II: the reactive-infiltration instability. Am. J. Sci. 287, 1008–1040.
Panga, M.K.R., Ziauddin, M., Balakotaiah, V., 2005. Two-scale continuum model for simulation of wormholes in carbonate acidization. AIChE J. 51, 3231–3248.
Scheidegger, A.E., 1974. The Physics of Flow through Porous Media. University of Toronto Press, Toronto.
Sherwood, J.D., 1987. Stability of a plane reaction front in a porous medium. Chem. Eng. Sci. 42, 1823–1829.
Zhao, C., Hobbs, B.E., Hornby, P., Ord, A., Peng, S., Liu, L., 2008. Theoretical and numerical analyses of chemical-dissolution front instability in fluid-saturated porous rocks. Int. J. Numer. Anal. Methods Geomech. 32, 1107–1130.
Zhao, C., Hobbs, B.E., Ord, A., 2009. Fundamentals of Computational Geoscience: numerical Methods and Algorithms. Springer, Berlin.
Zhao, C., Hobbs, B.E., Ord, A., 2013a. Theoretical analyses of acidization-dissolution front instability in fluid-saturated carbonate rocks. Int. J. Numer. Anal. Methods Geomech. 37, 2084–2105.
Zhao, C., Poulet, T., Regenauer-Lieb, K., Hobbs, B.E., 2013b. Computational modeling of moving interfaces between fluid and porous medium domains. Comput. Geosci. 17, 151–166.